Geoderma 197-198 (2013) 67–78

Contents lists available at SciVerse ScienceDirect

Geoderma

journal homepage: www.elsevier.com/locate/geoderma

Spatial patterns of soil total nitrogen and soil total phosphorus across the entire Loess Plateau region of China

Zhi-Peng Liu [a,c], Ming-An Shao [b,*], Yun-Qiang Wang [a,b,c]

[a] State Key Laboratory of Soil Erosion and Dry-land Farming on the Loess Plateau, Institute of Soil and Water Conservation, Chinese Academy of Sciences, Ministry of Water Resources, Yangling, Shaanxi 712100, PR China
[b] Key Laboratory of Ecosystem Network Observation and Modeling, Institute of Geographic Sciences and Natural Resources Research, Chinese Academy of Sciences, Beijing 100101, PR China
[c] University of Chinese Academy of Sciences, Beijing 100049, PR China

ARTICLE INFO

Article history:
Received 10 August 2011
Received in revised form 7 December 2012
Accepted 17 December 2012
Available online 28 January 2013

Keywords:
Spatial variability
Nitrogen
Phosphorus
Land use
Loess Plateau
Geostatistics

ABSTRACT

Soil total nitrogen (STN) and soil total phosphorus (STP), which vary spatially at different scales, play important roles in both agriculture and in the natural environment, especially those related to soil productivity and aquatic eutrophication. However, little information is available about the regional spatial availability of STN and STP and the influence of land use at the regional scale of the Loess Plateau (620,000 km^2) of China. Therefore, 764 soil samples were collected from 382 sampling sites across the region in order to determine STN, STP and other related soil properties and to relate them to site characteristics. Classical statistics and geostatistics were used to analyze the current status and spatial pattern of STN and STP. Mean STN and STP concentrations ranged from 0.50 g kg^{-1} to 0.81 g kg^{-1} and from 0.46 g kg^{-1} to 0.61 g kg^{-1}, respectively, under different land use types. Mean STN and STP densities ranged from 0.27 kg m^{-2} to 0.39 kg m^{-2} and from 0.27 kg m^{-2} to 0.38 kg m^{-2}, respectively, under different land use types. The concentrations and densities of STN and STP under different land use types were all moderately variable. Land use, precipitation and temperature significantly affected both STN and STP ($p<0.05$). The results varied among different precipitation and temperature regions for different land use types. Generally, cropland had higher concentrations and densities of STN and STP than forestland and grassland, and regions with higher precipitation and temperatures had higher STN and STP densities. Significant correlations were found between STN and STP, with selected variables, i.e. soil organic carbon, precipitation, temperature, elevation, latitude, longitude, slope gradient, clay content, silt content and soil pH. The results were not consistent within either STN, or STP, or the land use types. Therefore, land-use specific linear models were derived that predicted STN and STP. Both STN and STP demonstrated moderate spatial dependence. The spatial range of STN and STP ranged from 374 km to 461 km and from 546 km to 664 km, respectively, which were much greater than our sampling intervals (30–50 km). Distribution maps of STN and STP densities, derived by kriging interpolation, showed similar patterns with a central area of low values surrounded by bands of higher values progressively increasing towards the region's boundaries. Stocks of STN and STP were estimated to be 0.217 Pg and 0.205 Pg in the upper 0–40 cm soil layers, which were about 5.4% and 7.3% of the total nitrogen and phosphorus stocks in China. Our study suggests that it is important to take land use into account when considering variations of STN and STP at the regional scale. The spatial data of STN and STP could serve as initial inputs in regional nitrogen and phosphorus models and could be combined with soil erosion data to assess the risks of nitrogen and phosphorus losses to aquatic systems.

1. Introduction

Soil nitrogen (N) and phosphorus (P) play important roles in terrestrial ecosystem functions by affecting soil properties (Hati et al., 2008), plant growth (Quilchano et al., 2008) and soil microbial activities (Liu et al., 2010). Compared to other soil nutrients, both soil N and P are considered essential nutrients that most frequently limit soil productivity (Giesler et al., 2002). A number of biogeochemical processes, such as immobilization by recalcitrant organic matter and P adsorption by Fe and Al oxides, could reduce the biological availability of soil N and P (Moazed et al., 2010). Other processes, such as leaching and denitrification, may also lead to N losses from soil (Vitousek et al., 2002). In order to sustain crop yields, chemical fertilizers are widely applied to the topsoil in order to improve N and P levels in agricultural ecosystems. However, the undesirable and excess N and P can enter surface and ground water bodies through leaching, runoff and soil erosion, consequently leading to eutrophication of these aquatic ecosystems (Chen et al., 2008). Furthermore, soil N and P levels are closely correlated with soil organic carbon cycles (Bronson et al., 2004), which have dynamic effects on greenhouse gas emissions that are linked to global climate change (Lal, 2004). Thus, a better knowledge

* Corresponding author. Tel.: +86 29 87012405; fax: +86 29 87012334.
E-mail address: shaoma@igsnrr.a.cn (M.-A. Shao).

0016-7061/$ – see front matter. Crown Copyright © 2013 Published by Elsevier B.V. All rights reserved.
http://dx.doi.org/10.1016/j.geoderma.2012.12.011

of soil N and P levels and their distributions is necessary when evaluating current or potential soil productivity and assessing potential environmental pollution, as well as for a better understanding of climate change and its feedbacks (Jennings et al., 2009).

As major indicators of soil fertility and quality, soil total nitrogen (STN) and soil total phosphorus (STP) are generally used to represent the overall N and P levels in soil. Like other soil properties, STN and STP are distributed heterogeneously in soils, and the degree of variation is a function of the study scale and/or its aspects (e.g. support, spacing, and extent) (Wang et al., 2009). This spatial heterogeneity is caused by various factors (Jenny, 1941), which include climatic variables (Patil et al., 2010), parent material (Lin et al., 2009), topography (Rezaei and Gilkes, 2005), vegetation types (Rodríguez et al., 2009), soil texture (Gami et al., 2009) and land use (Ross et al., 1999; Wang et al., 2009). Among these factors, land use plays a more dynamic role in regulating spatial patterns of STN and STP, since land use change could occur more frequently due to both climate change and human activities, especially those resulting from large-scale policy interventions (Ostwald and Chen, 2006).

In the last decade, traditional statistics, in combination with geostatistics, have been widely applied to assess spatial variability of soil properties and their relationships with environmental factors, especially those associated with land use (Meersmans et al., 2008; Rodríguez et al., 2009; Wang et al., 2006, 2009, 2010). However, compared to soil organic carbon, soil N and P have received less attention and most studies on soil N and P spatial distributions have been conducted over small areas (Rodríguez et al., 2009; Wang et al., 2006, 2009). Information about the spatial variability of STN and STP and the effects of pertinent factors among different land use types is not currently adequate at larger scales, which limits the prediction of regional responses to large-scale environmental changes occurring when land use is altered, especially those resulting from national or regional policies. Therefore, it is necessary to investigate STN and STP at regional or national scales to optimize soil management and to avoid potential non-point source pollution, as well as to improve model accuracy by providing spatial input data for regional simulation models (Lin et al., 2009).

The Loess Plateau of China has deep loess deposits and undergoes intense soil erosion that makes it a fragile terrestrial ecosystem. Moreover, its location at the boundary between monsoon and non-monsoon zones makes the Plateau sensitive to global climate change (Ostwald and Chen, 2006). The soil erosion modulus has been reported to be 1000–15,000 t $km^{-2}a^{-1}$ in this region (Shi and Shao, 2000). Along with the eroded surface soil, a massive amount of soil N and P is transported into the Yellow River and finally into the marine ecosystem (Zheng et al., 2005), which leads to soil degradation and also water body pollution and eutrophication (Chen et al., 2008).

Remarkable land use changes have taken place in this oldest and important agricultural region of China during the last three decades. The land reform of 1982 (the "Household Responsibility System"), stimulated agricultural production in this region, and large areas of steep slopes where grassland or forests had grown were cultivated (Ostwald and Chen, 2006). However, the intensified agriculture and mismanagement increased environmental degradation, soil erosion and desertification (Liu, 1999). Since the 1990s, the Chinese government has initiated a series of environmental restoration and protection programs in this region, such as the "Grain-for-Green" project that aimed at decreasing cultivation on steep slopes by encouraging farmers to plant trees and grasses instead of grain crops. Clearly, these policy-driven land use changes could have greatly affected the content and spatial pattern of N and P in soils (Wang et al., 2009). Thus, from the perspectives of ecosystem research and environmental protection, it is important to know the spatial variability of STN and STP as affected by land use in the Loess Plateau region. Also, from a large-scale perspective, little information is available about the regional distribution patterns of STN and STP and how these are affected by environmental factors among different land use types across the entire Loess Plateau region.

Therefore, the objectives of our study were: (1) to investigate the current status and regional spatial variability of STN and STP in surface soils across the entire Loess Plateau region of China; (2) to analyze the relationships between STN and STP and selected environmental factors, and especially the effects of land use and climatic variables; (3) to provide an overview of the regional distributions of STN and STP and to calculate the regional stocks of STN and STP using a geostatistical method.

2. Materials and methods

2.1. Study area

The study area was the entire Loess Plateau (33°43′–41°16′N, 100°54′–114°33′E), which is located in northwestern China, between the upper and middle reaches of the Yellow River, covering a total area of 620,000 km^2, which is about 6.5% of the area of China (Fig. 1a). The region is dominated by a temperate, arid and semi-arid continental monsoon climate. The mean annual precipitation ranges from 150 mm in the northwest to 800 mm in the southeast, 55–78% of which falls between June and September, mostly in high intensity rainstorms. The

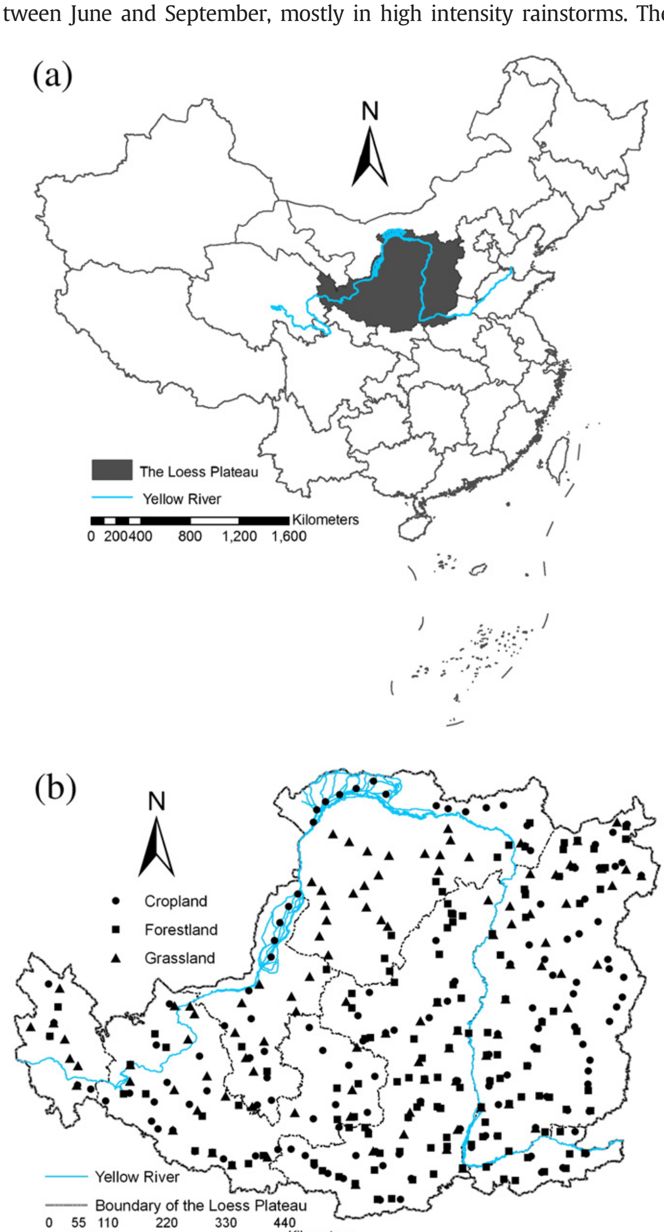

Fig. 1. Locations of the Loess Plateau region in China (a) and the sampling sites (b).

annual solar radiation ranges from 5.0×10^9 to 6.7×10^9 J m^{-2}. The mean annual temperature decreases from 3.6 to 14.3 °C along a northwest to southeast transect (Yang and Shao, 2000). The accumulated temperature above 0 °C is 3200–3900 °C. Surrounded by mountains, the loessial landforms include Yuan (a large flat surface with little erosion), ridges, hills and gullies at elevations ranging from 100 to 3000 m (Shi and Shao, 2000; Yang and Shao, 2000).

Loess–paleosol deposits cover most of the area and range from 30 to 80 m in thickness. The soils are mainly derived from loess, and are of diverse types, i.e. Hese soil, Lou soil, Heilu soil, Huangmian soil, Huigai soil, Ligai soil, Zonggai soil, Zongmo soil and Fengsha soil according to the Chinese taxonomic system (Gong, 2003). The most widespread soil is clay–loam in texture, with sandier soils in the northwest and clayier soils in the southeast (Wang et al., 2011). The natural vegetation has been largely destroyed by deforestation and cultivation. Vegetation type changes from southeast to northwest in the order of forest, forest-steppe, typical-steppe, desert-steppe, steppe-desert zones. The main land uses on the Plateau can be classified as cropland, grassland or forestland. Low vegetation coverage and intensive rainfall caused severe soil erosion in most parts of the Loess Plateau region (280,000 km^2) (Tang, 1991). A large quantity of the eroded mass is transported into the Yellow River, which carries a sediment load of about 16.4×10^9 t year^{-1} (Sediment Specialty Committee of Chinese Water Resources Association, 1989).

2.2. Field sampling and laboratory analysis

In order to obtain accurate STN and STP data, we conducted intensive soil sampling by investigating 382 sampling sites throughout the Loess Plateau region, from April to November, 2008 (Fig. 1b). We pre-selected the sampling routes across the region that would use the existing road transportation system, with a spacing distance between two adjacent routes of about 40 km. The sampling sites were generally designated along the selected sampling routes. The base interval between two adjacent sites was also designed to be 40 km. Additionally, a grid 40 km by 40 km was placed over a digital elevation map with a 90-m resolution overlying the selected road system for further guidance. During the field sampling, the actual approximate interval between sampling sites was 30–50 km because the logistical problem of accessing the sites had to be taken into account. The actual sample site was randomly selected to represent the main topography, land-uses and vegetation types within the range of vision. We used a global positioning system (GPS) receiver (eTrex venture, 5-m precision in the horizontal direction) to identify the site's longitude, latitude and elevation. At each site, notes were also made of the major land-use type (cropland, forestland, grassland), vegetation species and coverage by observation; aspect and slope were measured with a geological compass; and information on human activities (irrigation, fertilizer use and crop yield) was collected from surveys of the local inhabitants.

Disturbed soil samples were collected from two different soil layers, i.e., 0–20 cm and 20–40 cm, using a 5-cm-diameter soil auger in 10-cm increments down the soil profile. This procedure was repeated five times in places randomly located within a 10-m radius at each site; then all of the ten samples from a soil layer were mixed by hand to give one composite sample, which was taken to represent that soil layer at the sampling site. A total of 764 soil samples were collected to determine STN and STP concentrations and other soil properties. In addition, undisturbed soil cores from the 0–20 cm and 20–40 cm soil layers were collected to determine soil bulk density.

All disturbed soil samples were air-dried, crushed to pass through either a 0.25-mm or a 2-mm mesh for laboratory analysis. Soil total nitrogen concentration (g kg^{-1}) was analyzed using the Kjeldahl digestion procedure (Bremner and Tabatabai, 1972). Soil total phosphorus concentration (g kg^{-1}) was determined by alkaline digestion (NaOH 2 g, <0.25 mm soil 0.25 g, 400 °C–15 min and 720 °C–15 min) followed by molybdate colorimetric measurement (Murphy and Riley, 1962). Soil organic carbon was analyzed using the Walkley–Black method (Nelson and Sommers, 1982). Soil pH value was measured at a soil to water mass ratio of 1:1 using a pH meter equipped with a calibrated combined glass electrode (McLean, 1982). Undisturbed soil cores were oven dried at 105 °C for 10 h and then weighed to calculate soil bulk density (g cm^{-3}). Soil clay (<0.002 mm) and silt (0.002–0.05 mm) contents (%) were determined by laser diffraction using a Mastersizer 2000 particle size analyzer (Malvern Instruments, Malvern, England).

The precipitation and temperature datasets were derived as annual means of meteorological records (1951–2001) from 68 weather stations distributed throughout the region (Wang et al., 2011), and kriging interpolation was employed to create a continuous data surface of mean annual precipitation and mean annual temperature. Then the spatial coordinates of the sampling points were used to extract meteorological parameters for each sampling point from that data surface (Liu et al., 2011).

2.3. Calculation of densities and stocks of STN and STP

For an individual soil profile, with n layers, soil total nitrogen density (STND) and soil total phosphorus density (STPD) were calculated using the following equation (Liu et al., 2011):

$$STND \text{ or } STPD = \sum_{i=1}^{n}[L_i \times Con_i \times \rho_{bi} \times (1-F_i/100)]/100$$

where *STND* or *STPD* is the total amount of STN or STP between the soil surface and a given depth per unit area (kg m^{-2}); n is the number of layers considered in the given depth; i is the ith layer; Con_i is the STN or STP concentration (g kg^{-1}) in the ith layer; and Li, ρ_{bi}, and F_i are the thickness (cm), bulk density (g cm^{-3}), and the proportion (%) of coarse (>2 mm) fragments in the ith layer, respectively. The occurrence of coarse particles in the loess soils of the study region was rare, so F_i was considered to be negligible (Wang et al., 2010). In our study, we calculated STND and STPD to a depth of 40 cm using data from the two (0–20 cm and 20–40 cm) different soil layers.

We performed spatial interpolation using the ordinary kriging method to create STND and STPD surfaces, which covered the entire area of the Loess Plateau region. The surfaces were then exported as a raster layer with a defined resolution of 3000 m×3000 m, in which every grid square has a density value (kg m^{-2}) and an area value (m^2). Then, we calculated STN and STP stocks using the following equation (Liu et al., 2011):

$$STNS_h \text{ or } STPS_h = \sum_{i=1}^{n}\left(Dens_i \times Area \times 10^{-12}\right)$$

where $STNS_h$ or $STPS_h$ is the total STN or STP stock (Pg; 10^{15} g) at depth h in the study region; n is the total grid number of the raster; i is the ith grid square; $Dens_i$ is STN or STP density (kg m^{-2}) for the ith grid square calculated to depth h, and *Area* is the area (m^2) of each grid square, set by the defined resolution. In our study, the STNS or STPS was calculated for the upper 0–40 cm soil layer. These calculations were performed using the GIS software package Arcmap Desktop (version 9.1) with the Spatial Analyst module.

2.4. Statistical analysis

2.4.1. Classical statistics

The datasets were analyzed to determine the descriptive parameters, i.e., maximum, minimum, mean, median, standard deviation (S.D.), and coefficient of variation (C.V.). The Kolmogorov–Smirnov (K–S) method, together with skewness and kurtosis values, was used to evaluate the normality of the datasets. For data that failed the K–S test, a logarithmic or a square-root transformation was performed to achieve a normal distribution for use in further statistical analyses.

A two-sample *t*-test ($p<0.05$) was performed to detect significant differences between STN and STP in the upper (0–20 cm) and subsoil

(20–40 cm) layers. A one-way analysis of variance (ANOVA), followed by the Duncan's multiple comparisons test ($p<0.05$), was used to determine whether the means of STN or STP differed significantly under different land use types. Pearson correlation coefficients were used to determine the strength of relationships between STND and STPD, and the pertinent factors, i.e. soil organic carbon (SOC), precipitation (Pre), temperature (Tem), elevation (Elev), latitude (Lat), longitude (Longi), slope gradient (Slp), clay content (Clay), silt content (Silt) and soil pH. We used multivariate linear regression to further quantify the relationship and to make a general prediction of STND and STPD under different land use types. However, significant mutual correlations exist among all the explanatory variables. For example, precipitation and temperature decrease with increased elevation in our study region (Liu et al., 2011; Wang et al., 2011). Close relationships between SOC and clay and silt contents have been widely reported (Hassink, 1996). Precipitation and temperature also impact pH in soils. The existence of one variable in the regression model could affect the significance of other related variables. Given these many variables and complicated interactions, a stepwise method with a bidirectional elimination approach was used to automatically choose the predictive variables in the regression model. The significance level for the F-tests at each stage for entry and removal was 0.05, and no interaction was included.

Classical statistical analysis was carried out with R-studio (version 0.92.44), using the stats package (version 2.12.1).

2.4.2. Geostatistics

Based on the theory of regionalized variable (Matheron, 1963), geostatistics uses a semivariogram to quantify spatial autocorrelation and consequently to provide parameters for the optimal spatial interpolation, which is known as the kriging method (Webster and Oliver, 2000). The measured data was used to calculate the experimental semivariogram, which is then, fitted by authorized theoretical models, i.e. linear, Gaussian, spherical and exponential (Goovaerts, 1999). The best-fitted model was considered to be the one having the smallest residual sum of squares (RSS) and the largest coefficient of determination (R^2). Three major parameters could be derived from the fitted model, i.e. the nugget (C_0), the sill ($C+C_0$) and the range, which could identify the spatial structure of the variables at a given scale. The total variance (sill, $C+C_0$) is expressed as the summary of the structural variance (C, variance explained by spatial autocorrelation) and the nugget effect (C_0, variance occurring at a smaller scale than the field sampling and from the experimental error). To determine the magnitude of spatial dependence, the percentage of total variance (sill) explained by random variance (C_0) was calculated as a nugget to sill ratio. The spatial range represents the maximum distance within which variables show spatial dependence. In the kriging interpolation, the predictions are like weighted moving means, in which the weights are determined by the autocorrelation to achieve unbiased error and minimum estimation variance. Details of the calculation of the semivariogram and kriging interpolation are published elsewhere (Goovaerts, 1999; Webster and Oliver, 2000). In our study, ordinary kriging was used for the spatial interpolation of the densities of STN and STP in the 0–40 cm soil layers across the Loess Plateau region. Leave-one-out cross-validation was then performed to check the interpolation quality. Mean error (ME), the root-mean squared-error (RMSE) and the mean standardized error (MSE) were calculated as follows:

$$ME = \frac{1}{n}\sum_{i=1}^{n}(P_i - M_i)$$

$$RMSE = \sqrt{\frac{1}{n}\sum_{i=1}^{n}(P_i - M_i)^2}$$

$$MSE = \frac{1}{n}\sum_{i=1}^{n}[(P_i - M_i)/\sigma_i]$$

where n is the number of the locations; P_i and M_i are the predicted and measured values at location i, respectively; σ_i is the kriging standard error at location i.

The geostatistical analysis was performed with the GS+ software (version 7.0) and the distribution map was produced with ArcGIS desktop software (version 9.2).

3. Results and discussion

3.1. Descriptive statistics

In our study, both concentration and density values were used to represent the status of STN and STP on the Loess Plateau region. Descriptive statistical parameters of STN and STP under different land use types are shown in Table 1. In 0–20 cm soil layers, mean STN concentrations (STNC) and STP concentrations (STPC) ranged from 0.58 g kg^{-1} to 0.81 g kg^{-1} and from 0.50 g kg^{-1} to 0.73 g kg^{-1}, respectively, under the different land use types. In 20–40 cm soil layers, mean STNC and STPC values ranged from 0.46 g kg^{-1} to 0.60 g kg^{-1} and from 0.48 g kg^{-1} to 0.61 g kg^{-1}, respectively. For all 382 soil samples, the raw STNC and STPC data for both soil layers were normally distributed (K–S test $p>0.05$) after log-transformation (Table 1). The raw STND and STPD data for the 0–40 cm soil layer were normally distributed. The results of the normality test for concentration and density values of STN and STP under different land use types are shown in Table 1. For the *t*-test, ANOVA and multiple linear regression, a log or square-root transformation was carried out where necessary so that all datasets met the normality requirements.

The *t*-test showed that STNC and STPC were significantly higher ($p<0.05$) in 0–20 cm soil layers than that in 20–40 cm soil layers under all the land use types, except for the STPC under forestland and grassland (Fig. 2a). This could be attributed to the accumulation of litterfall and fertilizers as the main nitrogen source in these surface soil layers. Unlike nitrogen, or organic carbon, soil phosphorus is primarily derived from rock phosphate. Forestlands and grasslands received little additional anthropogenic P input in the surface soil, so that no significant difference in STPC was found between the upper soil layers and the subsoil layers. In contrast, croplands had significantly higher P content in the surface soil, which reflected the effect of agricultural activities.

For both soil layers, mean STNC were significantly higher ($p<0.05$) under croplands than under grasslands, while no significant difference in STNC was detected between cropland and forestland soils. Mean STPC in both soil layers increased under the different land uses in the order: croplands > forestlands > grasslands.

We calculated STND and STPD down to 40 cm soil depth. Mean STND and STPD were found to be 0.35 kg m^{-2} and 0.33 kg m^{-2} under mixed land uses, ranging from 0.27 kg m^{-2} to 0.39 kg m^{-2} and from 0.27 kg m^{-2} to 0.38 kg m^{-2}, respectively, under different land use types. In the whole of China, the mean STND and STNP in 0–40 cm soil layers have been reported to range from 0.08 kg m^{-2} to 2.17 kg m^{-2} and from 0.19 kg m^{-2} to 2.83 kg m^{-2} among different soil types, respectively (Yang et al., 2007; Zhang et al., 2005). Thus, the Loess Plateau region had a relatively low level of STND and STPD in China.

The ANOVA and post hoc tests showed that the effect of land use types on the STND and STPD was significant ($p<0.05$) and that the mean STND and STPD values increased in the order: croplands > forestlands > grasslands (Fig. 2b). Moreover, all the maximum values for the concentrations and densities of STN and STP occurred under cropland while all the minimum values occurred under forestland or grassland. The high values of STN and STP under cropland were consistent with other studies on the Loess Plateau (Wang et al., 2009) and this could be attributed to the application of organic and inorganic NPK fertilizers.

Table 1
Summary statistics for soil total nitrogen and soil total phosphorus under different land use types across the Loess Plateau, China.

Land use	Variable	Depth (cm)	Max.	Min.	Mean	Median	S.D.	C.V. (%)	Skewness	Kurtosis	D.T.
Cropland (n = 153)	STNC (g kg^{-1})	0–20	3.82	0.21	0.81	0.79	0.38	46.6	3.26	23.73	N.
		20–40	2.91	0.13	0.60	0.57	0.30	50.9	2.98	20.03	N.
	STPC (g kg^{-1})	0–20	2.79	0.30	0.73	0.68	0.26	35.6	3.89	25.02	L.N.
		20–40	1.04	0.31	0.61	0.61	0.11	18.3	0.42	1.75	N.
	STND (kg m^{-2})	0–40	1.92	0.11	0.39	0.38	0.19	48.4	3.28	24.49	N.
	STPD (kg m^{-2})	0–40	1.14	0.20	0.38	0.36	0.11	28.3	3.15	17.95	L.N.
Forestland (n = 128)	STNC (g kg^{-1})	0–20	3.36	0.05	0.77	0.71	0.53	68.6	2.29	8.04	S.N.
		20–40	2.54	0.03	0.53	0.54	0.32	59.8	2.27	11.98	N.
	STPC (g kg^{-1})	0–20	1.98	0.22	0.60	0.59	0.22	37.3	2.04	9.99	L.N.
		20–40	2.26	0.19	0.55	0.55	0.22	40.5	3.61	24.85	S.N.
	STND (kg m^{-2})	0–40	1.25	0.03	0.34	0.33	0.19	55.6	1.35	3.84	N.
	STPD (kg m^{-2})	0–40	0.88	0.14	0.31	0.29	0.10	33.2	1.86	6.89	N.
Grassland (n = 101)	STNC (g kg^{-1})	0–20	2.33	0.08	0.58	0.52	0.36	61.5	1.85	5.57	S.N.
		20–40	2.12	0.05	0.46	0.39	0.34	72.5	2.53	8.26	S.N.
	STPC (g kg^{-1})	0–20	1.05	0.17	0.50	0.53	0.15	31.1	0.17	1.13	N.
		20–40	0.90	0.16	0.48	0.51	0.15	30.5	0.14	0.39	N.
	STND (kg m^{-2})	0–40	0.97	0.04	0.28	0.25	0.16	58.1	1.91	4.89	L.N.
	STPD (kg m^{-2})	0–40	0.54	0.11	0.27	0.27	0.07	26.4	0.54	1.90	N.
Mixed land use (n = 382)	STNC (g kg^{-1})	0–20	3.82	0.05	0.74	0.68	0.44	59.5	2.49	12.4	L.N.
		20–40	2.91	0.03	0.54	0.51	0.32	59.3	2.48	12.9	L.N.
	STPC (g kg^{-1})	0–20	2.79	0.17	0.63	0.59	0.24	38.1	2.79	18.8	L.N.
		20–40	2.26	0.16	0.56	0.55	0.17	30.4	2.56	24.2	L.N.
	STND (kg m^{-2})	0–40	1.92	0.03	0.35	0.32	0.19	54.4	2.22	13.27	N.
	STPD (kg m^{-2})	0–40	1.14	0.11	0.33	0.30	0.11	32.8	2.10	11.28	N.

Notes: STNC, soil total nitrogen concentration; STND, soil total nitrogen density (0–40 cm); STPC, soil total phosphorus concentration; STPD, soil total phosphorus density (0–40 cm); n, number of samples; S.D., standard deviation; C.V., coefficient of variance; D.T., distribution type (normality test at p = 0.05); N., normal distribution; L.N., log-normal distribution; S.N., square-root-normal distribution.
Mixed land use refers to all land use types combined.

The coefficient of variation (CV) was used as an index to present the overall variation of STN and STP. The CV values for the concentrations and densities of STN and STP varied from 18.3% to 72.5% (Table 1), which all indicated moderate variation (Nielsen and Bouma, 1985). No apparent differences in CV values were found for STN or STP in the different soil layers and under the various land use types. Notably, STN CV values were 50% higher than those of STP CV. Others have also reported moderate variability of STN and STP at various scales (Lin et al., 2009).

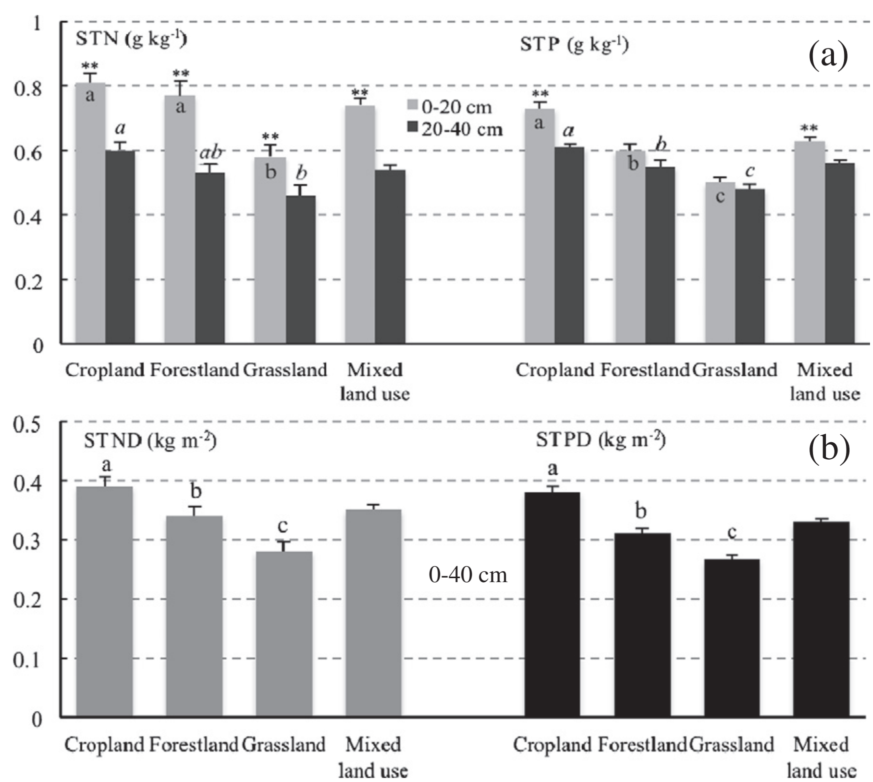

Fig. 2. Soil total nitrogen and soil total phosphorus concentrations (a) and densities (b) in different soil layers and under different land use types. The symbol ** above the bars denotes a significant difference between different soil layers under the same land use; different bold or italic letters above the bars of a particular soil layer denote significant differences between land use types for that layer. The error bars denote the standard error of the mean.

3.2. Correlation analysis

Pearson correlation coefficients between STND and STPD, and selected environmental factors are shown in Table 2. Under all land use types, STND was significantly ($p<0.05$) and positively correlated with STNP. For both STND and STPD, significant ($p<0.05$) and positive correlations were found with SOC, temperature, precipitation and clay content, while significant ($p<0.05$) and negative correlations were found with elevation, latitude, longitude, slope gradient and soil pH. Wang et al. (2009) reported similar correlations between STN and STP, with soil properties and topographical variables under different land use types in a small catchment on the north Loess Plateau. Positive correlations between STND and STPD, and climatic variables (i.e. precipitation, temperature) were also found in other large-scale studies in China (Lin et al., 2009; Yang et al., 2007).

However, the correlation coefficients were not consistent within either the variable or the land use types. For example, silt content showed significant ($p<0.05$) positive relationships with both STND and STPD under forestland and grassland, but a negative relationship under cropland. Slope gradient was significantly ($p<0.05$) correlated with STND only under cropland, and its correlation with STPD was not significant only under grassland. Elevation was only significantly ($p<0.05$) correlated with STND under grassland, and with STPD under forestland. Notably, no significant correlation was found between STND and STNP, with precipitation, temperature and elevation under cropland. It indicated that factors related to agriculture, such as tillage, compaction, irrigation and fertilization, probably play more important roles than natural factors in affecting STND and STPD in agriculture ecosystems.

3.3. Multivariate regression analysis

Multivariate linear regression using a step-wise method was performed to quantify the relationship between STND and STPD, with all the selected environmental factors under different land use types. The summaries of the linear regression models are shown in Table 3. In mixed land use, six variables: SOC, Silt, pH, Ele, Lat and Longi, were selected as significant ($p<0.05$) predictive variables in the linear model, and together they explained 79% of the variation in STND. To predict STPD, SOC, Clay, pH, Ele, Longi and Slp, were selected as significant ($p<0.05$) predictive variables, and together they explained 37% of the variation in STPD. Based on the correlation results (Table 2), it was concluded that these relationships between STND and STPD, were land use specific. Similarly, Tan et al. (2004) and Meersmans et al. (2008) constructed different linear regression models for different land use types in order to predict SOC content using several soil and topographic properties. In our study, land use was accounted for in the regression model in order to obtain a more comprehensive estimation of STND and STPD compared to the one mean mixed land use approach.

For both STND and STPD, the models under different land use types varied in their input parameters and coefficients (Table 3). For example, slope gradient and pH were included in the models for both STND and STPD under forestland, but not under cropland and grassland. Precipitation was considered to be an important predictive variable for STPD under grassland and forestland, but not under cropland. Elevation was only included in the model for STND under cropland. Under grassland, only two variables were needed to obtain accurate predictions of STND, indicated by a high determination coefficient (R^2) and a low root mean squared error (RMSE). Clearly, using land-use specific models could improve the predictions of STND and STPD. For STND, the R^2 of regression models increased from 0.79 under mixed land use to 0.92 under both forestland and grassland. For STNP, the model under grassland had a higher R^2 and a lower RMSE than those under mixed land use (Table 3). Using the selected variables, the models for STND had higher R^2 values than those for STPD under mixed land use types. The ANOVA showed that more than 50% of the explained variance of STND was contributed by SOC and this could be attributed to the strong relationship between SOC and STN (Table 2), which are closely linked in the biogeochemical processes in soils (Hagedorn et al., 2003). In contrast to STND, clay and silt contents contributed about 23% of the total explained variance, while SOC only accounted for 5% of the variance. The significant correlations between STPD under all land use types are presented in Table 2. Clay content was included in all the models for STPD under different land use types (Table 3). Similar results were also reported for STP in small-scale studies on the Loess Plateau (Wang et al., 2009). Moreover, the relatively low R^2 for STPD suggested that some other factors affecting STP status should be included in the model, such as parent material, soil erosion and land management practices (Chen et al., 2008; Smil, 2000).

3.4. Effects of precipitation and temperature

Regional and local climate changes have been reported across the Loess Plateau region (Hageback et al., 2005). Based on the climatic data from 1951 to 2001, a slight decrease in precipitation and an increase in temperature were found in different climate regions on the Loess Plateau (Wang et al., 2011). Between 1970 and 2000, in the northern part of the region, a 14%–19% decrease (1.8–2.6 mm/year) in annual precipitation as well as a 1 °C increase in annual temperature were recorded (Ostwald and Chen, 2006). This climate change could essentially influence water and heat balances, plant growth, land use policy and soil management, consequently impacting the spatial patterns and

Table 2
Pearson correlations between soil total nitrogen density (STND) and soil total phosphorus density (STPD) in 0–40 cm soil layers across the Loess Plateau, China.

Variable	Cropland (n = 153)		Forestland (n = 128)		Grassland (n = 101)		Mixed land use (n = 382)	
	STND	STPD	STND	STPD	STND	STPD	STND	STPD
STND (kg m^{-2})	1.000	0.561**	1.000	0.374**	1.000	0.412**	1.000	0.495**
STPD (kg m^{-2})	0.561**	1.000	0.374**	1.000	0.412**	1.000	0.495**	1.000
SOC (g kg^{-1})	0.823**	0.484**	0.940**	0.268**	0.856**	0.372**	0.912**	0.407**
Precipitation (mm)	0.030	0.074	0.431**	0.459**	0.203*	0.574**	0.212**	0.286**
Temperature (°C)	0.091	0.073	0.360**	0.356**	0.033	0.146	0.198	0.230**
Elevation (m)	0.116	−0.066	−0.072	−0.365**	−0.341**	−0.143	0.062	−0.208**
Latitude (°)	−0.209**	−0.123	−0.505**	−0.483**	−0.339**	−0.476**	−0.354**	−0.340**
Longitude (°)	−0.279**	−0.292**	−0.100	−0.065	−0.260**	−0.038	−0.196**	−0.065
Slope (°)	−0.247**	−0.207*	0.090	−0.231**	0.124	0.048	−0.025	−0.230**
Clay (%)	0.482**	0.392**	0.487**	0.453**	0.654**	0.467**	0.521**	0.515**
Silt (%)	−0.426**	−0.435**	0.297**	0.279**	0.506**	0.523**	0.219**	0.264**
pH (−)	−0.402**	−0.064	−0.599**	−0.423**	−0.455**	−0.389**	−0.514**	−0.358**

Notes: SOC, soil organic carbon; mixed land use refers to all land use types combined.
* Correlation is significant at the 0.05 level (2-tailed).
** Correlation is significant at the 0.01 level (2-tailed).

Table 3
Land-use specific linear regression models of soil total nitrogen density (STND) and soil total phosphorus density (STPD) in 0–40 cm soil layers across the Loess Plateau, China.

Land use	Dependent variable	Model structure	RMSE	R^2
Cropland (n = 153)	STND	STND = 1.200 + 0.311(SOC[a])** + 0.0007(Clay)* + 0.0026(Silt)* − 0.001(Ele[b])** − 0.015(Longi)**	0.10	0.73
	STPD	STPD[a] = 1.176 + 0.149(SOC[a])** + 0.002(Clay)** − 0.008(Silt)** − 0.018(Longi)**	0.19	0.34
Forestland (n = 128)	STND	STND = 0.054 + 0.028(SOC)** + 0.002(Clay)** − 0.059(pH)** + 0.004(Tem)* − 0.001(Slp)*	0.05	0.92
	STPD	STPD = 1.404 + 0.0007(SOC)** + 0.0015(Clay)** − 0.059(pH)** + 0.0004(Pre)** − 0.007(Longi)* − 0.002(Slp)**	0.08	0.36
Grassland (n = 101)	STND	STND[a] = − 2.994 + 0.835(SOC[a])** + 0.009(Clay)**	0.16	0.92
	STPD	STPD = 0.340 + 0.011(SOC[a])** + 0.001(Clay)** − 0.001(Silt)** + 0.0002(Pre)** − 0.007(Lat)*	0.05	0.50
Mixed land use (n = 382)	STND	STND = 1.965 + 0.247(SOC[a])** + 0.002(Silt)** − 0.077(pH)** − 0.001(Ele[b])** + 0.003(Lat)** − 0.013(Longi)**	0.09	0.79
	STPD	STPD = 1.542 + 0.055(SOC[a])** + 0.002(Clay)** − 0.021(pH)** − 0.004(Ele[b])** − 0.009(Longi)** − 0.002(Slp)**	0.09	0.37

Notes: SOC, soil organic carbon; Ele, elevation; Longi, longitude, Lat, latitude; Pre, precipitation; Tem, temperature; Slp, slope.
RMSE, root mean squared error; R^2, coefficient of determination. Mixed land use refers to all land use types combined.
* Significant at the 0.05 level (2-tailed).
** Significant at the 0.01 level (2-tailed).
[a] Data was logarithm transformed.
[b] Data was square-root transformed.

variability of nitrogen and phosphorus in soils. Therefore, it is necessary to know the effects of precipitation and temperature on STN and STP, especially in large-scale regions.

In our study, for each land use type, we compared STND and STPD under different precipitation and temperature regions (Section 2.4). The results of ANOVA and post hoc tests are shown in Fig. 3 (italic letters below the box-plots). Under cropland, no significant differences in STND and STPD were detected among different precipitation and temperature regions. It indicated that anthropogenic activities, such as cultivation, irrigation, fertilization and crop management, played an overwhelming role in affecting both STND and STPD in agricultural ecosystems. This effect may cover-up or offset the heterogeneity caused by climatic variables. Under forestland, STND was significantly ($p<0.05$) lower in regions with mid-range precipitation (250–500 mm) and temperatures (5–10 °C). No significant differences were found for STND in regions with high and low precipitation (<250 mm and >500 mm), and the same pattern was found in relatively high and low temperature (<5 °C and >10 °C) regions. In contrast to STND, STPD was significantly ($p<0.05$) higher in regions with high precipitation (>500 mm) and temperature (>10 °C). Under grassland, precipitation had significantly ($p<0.05$) positive effects on both STND and STPD, while the effect of temperature on STND was not significant. Furthermore, significantly ($p<0.05$) higher STPD was found in high temperature (>10 °C) regions.

Similar observations about the positive effect of precipitation on STN and STP have been reported elsewhere (Lin et al., 2009; Wang et al., 2005). Increased precipitation leads to an increase in vegetation productivity and N input to the soil. This effect could be more apparent in arid and semi-arid regions, because plant growth would be mainly limited by water supply (Yang et al., 2007). Temperature is another important factor affecting the N balance between input from litterfall and outputs through microbial decomposition (Post et al., 1985). Similarly, P can be more readily weathered and released from rocks under high precipitation and temperature conditions (Lin et al., 2009). However, the results showed that the effects of precipitation and temperature on STND and STPD were not consistent under different land use types (Fig. 3). It indicated that it is important to take land use type into account when considering the effects of climate change on STN and STP.

Additionally, we compared STND and STPD under different land use types for an individual precipitation and temperature region. The results are shown in Fig. 3 with significant difference indicated by the bold letters above the boxes.

In the regions with precipitation less than 500 mm, STND under cropland was significantly ($p<0.05$) higher than those under forestland and grassland (Fig. 3a). The lower STND under forestland and grassland could be attributed to the relatively lower biomass productivity due to the limited water supply in these arid and semiarid regions (Yang and Shao, 2000; Yang et al., 2007). In contrast, the higher STND under cropland could be explained by the anthropogenic nitrogen input through chemical or organic fertilizers (Zhang et al., 2006).

In the regions with precipitation greater than 500 mm, STND was significantly ($p<0.05$) higher under grassland, while no difference was detected between STND under cropland and forestland. Increased precipitation leads to better plant growth and more nitrogen input through litterfall and, consequently, to higher STND. Grasslands appeared to be more sensitive to this positive effect of precipitation. In all precipitation regions, croplands were found to have significantly ($p<0.05$) higher STPD, while no significant difference was detected between the forestlands and the grasslands. The same pattern was also found for STPD in the regions with temperatures less than 10 °C and for STND in regions with temperatures between 5 and 10 °C (Fig. 3b). These results indicated that human activity, especially fertilization, could greatly increase STPD in cropland. However, this land use effect was neither significant for STND in the region with low temperatures (<5 °C) nor for STPD in the region with high temperatures (>10 °C) (Fig. 3b). Low temperatures can limit microbial decomposition of organic matter (Karhu et al., 2010), leading to accumulation of organic carbon and nitrogen in soils (Leifeld et al., 2005). In contrast, high temperatures could enhance weathering processes and activities of soil microorganisms, which may lead to more P being released from the parent material (Lin et al., 2009). On the Loess Plateau, these factors may be more influential under forestland and grassland than that under cropland. The comparative higher STND and STPD under cropland, which were found in other regions, were not detected in the cold regions (<5 °C) for STND and warm regions (>10 °C) for STPD (Fig. 3b). Moreover, other factors, such as soil clay content, soil pH, soil erosion and their interactions with precipitation and temperature, could also play important roles in affecting STND and STPD in different climatic regions.

3.5. Geostatistical analysis

3.5.1. Semivariogram and spatial autocorrelation

Experimental semivariograms were calculated for the concentration (0–20 cm, 20–40 cm) and density (0–40 cm) values of STN and STP. As shown in Table 4, all the datasets showed weak directional variation, which was indicated by the anisotropy ratios that were less than 2.5 (Trangmar et al., 1985). Thus, isotropic semivariograms of STN and STP were calculated and fitted by each of the four theoretical models. In our study, the experimental semivariograms were best fitted by either the Gaussian model or the spherical model (Fig. 4). The parameters derived from the models (i.e. the nugget, the sill and the range) are shown in Table 4. The nugget to sill ratios ranged from 35.3% to 49.9%, which indicated that both the concentration and density of STN and STP had moderate spatial dependence (Cambardella et al.,

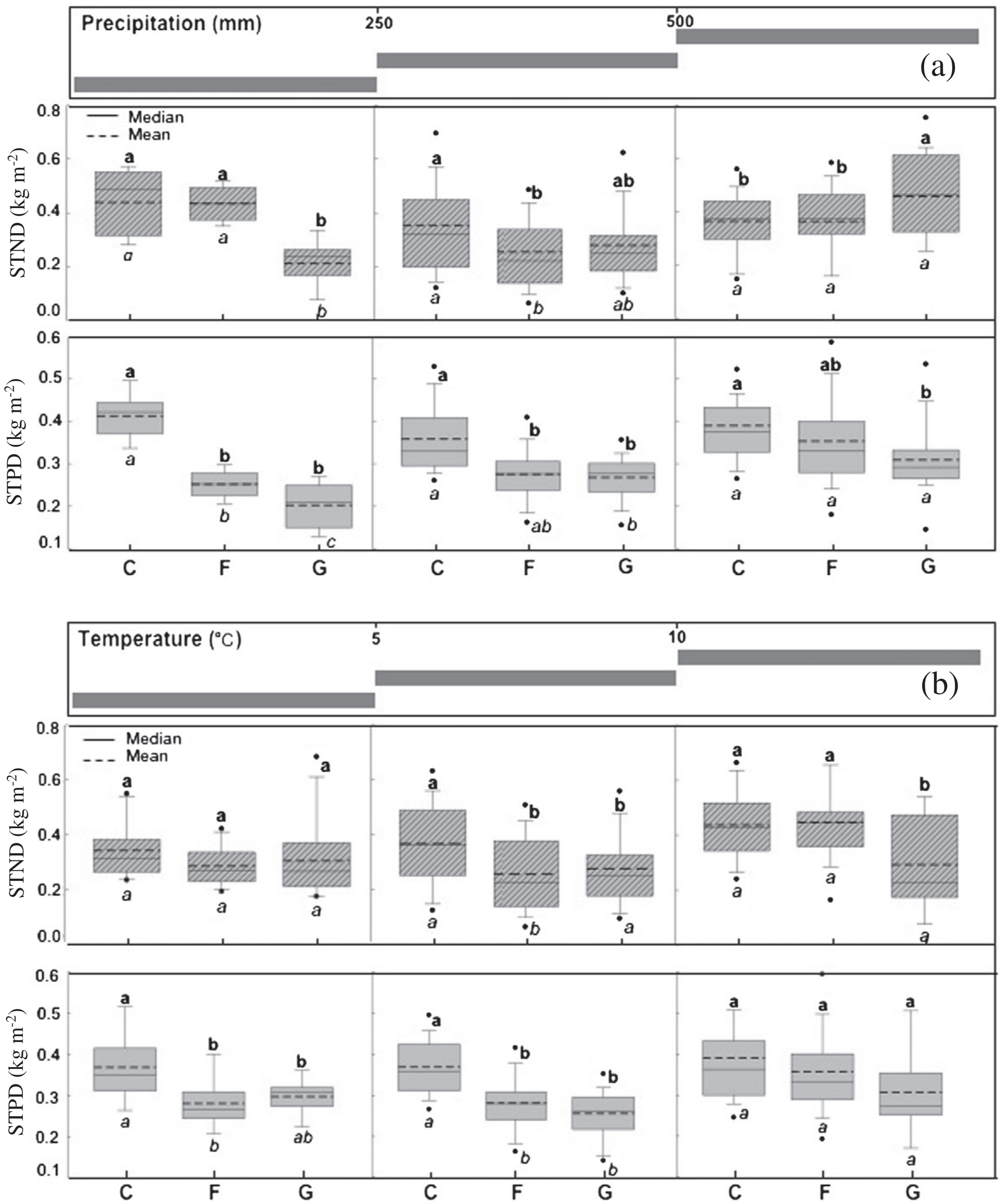

Fig. 3. Soil total nitrogen density (STND kg m^{-2}) and soil total phosphorus density (STNP kg m^{-2}) in 0–40 cm soil layers within different (a) precipitation-based and (b) temperature-based regions and under different land use types. Different bold letters above the boxes denote significant differences between different land use types within a box-plot (C, cropland; F, forestland; G, grassland); different italic letters below the boxes denote significant differences between different precipitation or temperature regions for a given land use type. One-way ANOVA ($p<0.05$) and Duncan's multiple range test ($p<0.05$) were used.

1994). This dependence was derived from the intrinsic systematic variation of soil properties and environmental factors, such as parent material, soil texture, precipitation, temperature, topography, vegetation and human activities (Jenny, 1941; Liu et al., 2011; Wang et al., 2009).

From the regional perspective, the spatial range of STN varied from 374 km to 461 km, which was smaller than that of STP (546–800 km), which indicated that STP had spatial dependence within a larger separation distance. Notably, the spatial range was much larger than our sampling interval (30–50 km), which demonstrated that our sampling system was adequate for detecting the spatial patterns of STN and STP at the regional scale (Garten et al., 2007). The range of density values was larger than that of concentration values for both STN and STP, suggesting that soil bulk density may have a weaker spatial variability than STNC and STPC given the relationships between bulk density and these values described in Section 2.3. Moreover, the spatial ranges of STNC and STPC, in the upper soil layers, were slightly smaller than those in the subsoil layers, which may indicate greater heterogeneity in the upper soil layers. This could be attributed to the greater random variance resulting from both natural processes and human disturbances that mainly affected the surface soil layer (Cambardella et al., 1994).

Table 4
Geostatistical parameters of soil total nitrogen and soil total phosphorus in 0–40 cm soil layers across the Loess Plateau, China.

Variable	Depth (cm)	Model	R^2	Nugget (C_0)	Sill ($C+C_0$)	Range (km)	Nugget/sill ratio (%)	Anisotropy ratio (–)
STNC	0–20[a]	Gaussian	0.96	0.158	0.447	374	35.3	2.32
	20–40[a]	Gaussian	0.98	0.184	0.417	400	44.2	2.28
STND	0–40	Gaussian	0.97	0.017	0.034	461	49.9	1.37
STPC	0–20[a]	Gaussian	0.98	0.071	0.172	546	40.2	1.69
	20–40[a]	Gaussian	0.97	0.054	0.130	580	41.6	1.93
STPD	0–40	Spherical	0.93	0.007	0.014.	800	49.9	1.95

Notes: STNC, soil total nitrogen concentration; STND, soil total nitrogen density; STPC, soil total phosphorus concentration; STPD, soil total phosphorus density; R^2, coefficient of determination.

[a] Data was logarithm transformed.

3.5.2. Spatial distribution of STN and STP

Using the input parameters derived from the fitted semivariograms, kriging interpolation was used to obtain spatial distribution maps of STND and STPD across the Loess Plateau region (Fig. 5). Predicted values were plotted against measured values to check the interpolation quality (Fig. 6). Most of the paired points in the middle range were close to the 1:1 line, indicating that both STND and STNP were well predicted in this range. The interpolation also showed a centralization effect, since small values were overestimated and large values were underestimated (Fig. 6). This is the commonly observed smoothing effect inherent in the ordinary kriging estimation method as well as in any other estimation based on a weighted average (Yamamoto, 2005).

The cross-validation determined that the mean error, the root-mean squared-error, and the mean standardized error were −0.0001, 0.143, 0.002 and 0.0003, 0.092, 0.001 for STND and STPD, respectively. These values were reasonably low and close to 0, which indicated that the interpolation was reliable and the distribution maps could be used to represent the regional spatial patterns of STND and STPD (Issaks and Srivastava, 1989).

In Fig. 5, STND and STPD demonstrated substantial spatial variation across the Loess Plateau region. Generally, both variables had a similar overall spatial pattern, characterized by a center area with low STND or STPD values surrounded by bands with higher values that progressively increased outwards towards the region's boundaries. Low STND values were apparent in the areas along the Yellow River between Shanxi and Shaanxi provinces, where soil erosion was most severe on the Loess Plateau (Tang, 1991). Low vegetation coverage and limited input biomass, together with the loss of large amounts of eroded surface soil can lead to low STND in these areas. Moreover, STND had highly similar distribution patterns compared

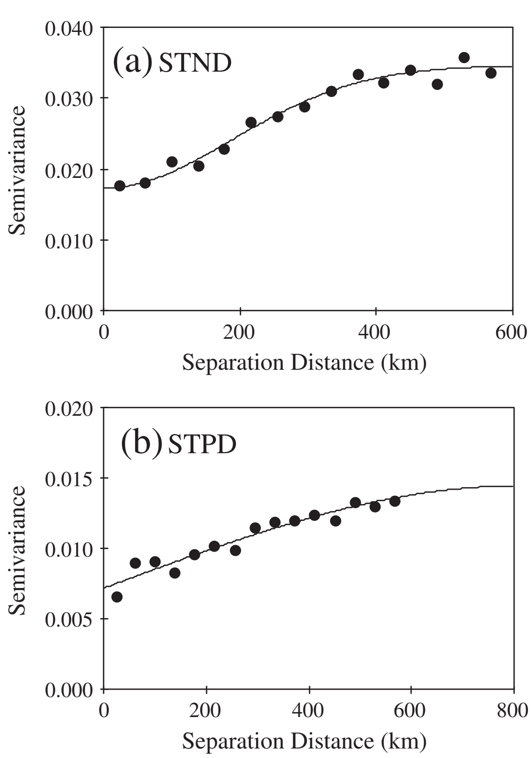

Fig. 4. Experimental semivariograms and the best fitted models for (a) soil total nitrogen density (STND) and (b) soil total phosphorus density (STPD) in 0–40 cm soil layers across the Loess Plateau, China.

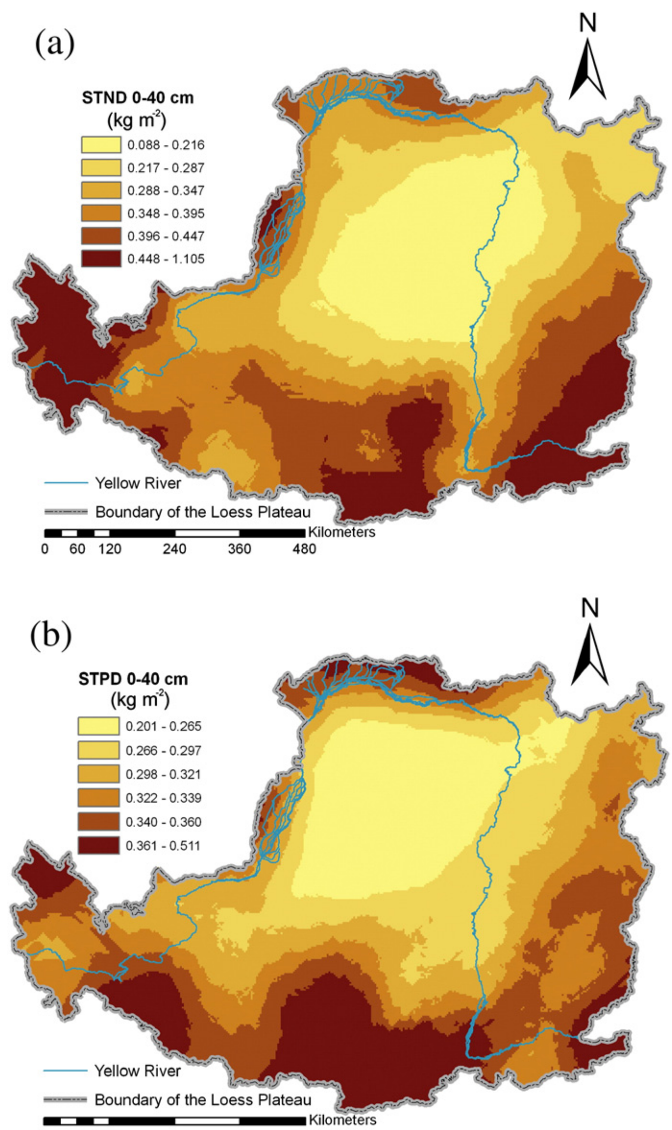

Fig. 5. Spatial distribution maps of (a) soil total nitrogen density (STND kg m^{-2}) and (b) soil total phosphorus density (STPD kg m^{-2}) in 0–40 cm soil layers across the Loess Plateau, China.

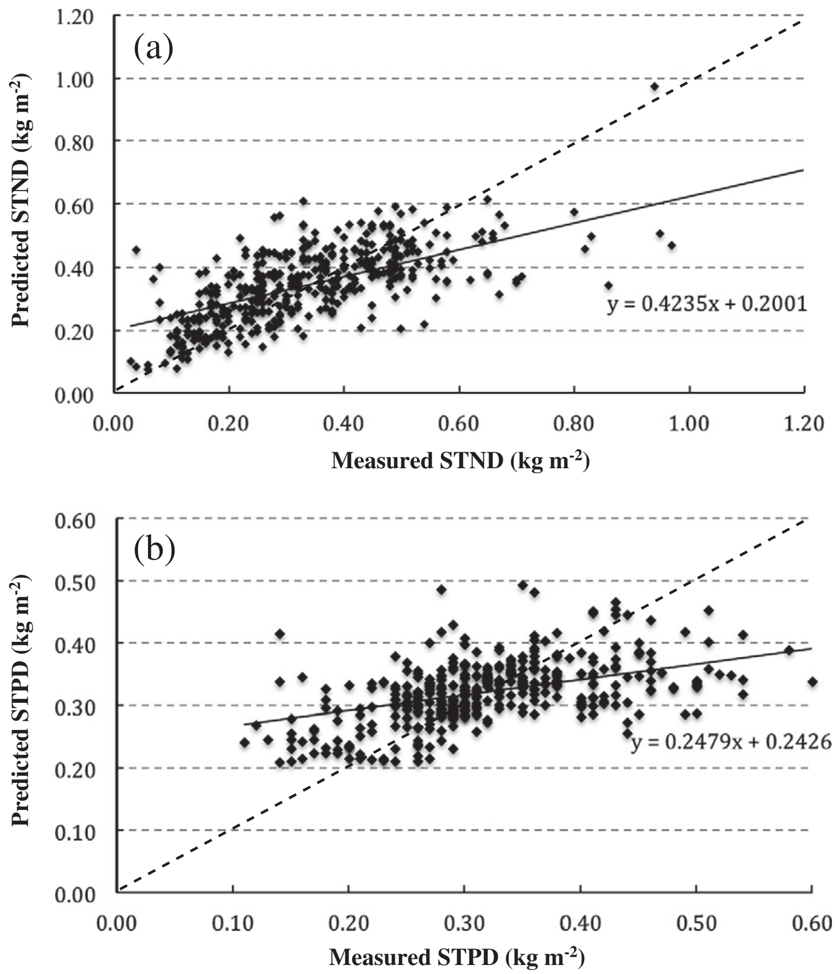

Fig. 6. Cross-validation of kriging interpolation of (a) soil total nitrogen density (STND kg m^{-2}) and (b) soil total phosphorus density (STPD kg m^{-2}) in 0–40 cm soil layers across the Loess Plateau, China (dashed line denotes a 1:1 line).

to those reported for SOC density (Liu et al., 2011), which also demonstrated the close relationship between STN and SOC. Areas with the lowest STPD were located in the northwestern part, where the sandy Ordos Plateau is located. Relatively higher STND and STPD values were found in the western and southeastern areas. However, some differences in the detailed spatial patterns can be detected between STND and STPD.

Although kriging interpolation is considered to be the best-unbiased method, the smoothing effect should be considered when interpreting these results because the lower values were underestimated and the higher values were overestimated to some extent. The kriging method converted finite discrete point data to continuous surface data so that there were values for every possible location in the region. This spatial data could be useful as the initial state input into regional nitrogen and phosphorus models to increase their accuracy. Moreover, the spatial distribution maps could also be combined with soil erosion data and transformation models to evaluate the risks of nitrogen and phosphorus losses into the aquatic system.

3.5.3. Regional stocks of STN and STP

Finally, we calculated the regional STN and STP stocks, using the accumulative process (see Section 2.4). According to our data, there were 0.217 Pg STN and 0.205 Pg STP stored in the upper 0–40 cm soil layers across the Loess Plateau. In the whole of China, STN stocks have been estimated to be 7.4 Pg–8.3 Pg (Tian et al., 2006; Yang et al., 2007) in the 0–100 cm soil layers, which would be about 5.6% of the global soil N storage (Batjes, 1996). In the 0–50 cm soil layers, based on the data from China's Second National Soil Survey (1979–1983), the STN and STP stocks were calculated to be 4.973 Pg (Yang et al., 2007) and 3.500 Pg (Zhang et al., 2005), respectively. In order to compare the results, we assumed vertical homogeneity of STN and STP stocks in the upper soils and multiplied our results by a factor of 1.25 to represent the STN and STP stocks in the 0–50 cm soil layers. Thus, we concluded that the Loess Plateau held about 5.4% and 7.3% of China's STN and STP stocks in the upper 0–50 cm soil layers, respectively.

4. Conclusion

We analyzed the current status and regional spatial variability of STN and STP, using the measured data from 382 locations across the Loess Plateau region. The results showed that the Loess Plateau had low levels of both STN and STP compared with the whole of China. The concentrations and densities of STN and STP under different land use types were all moderately variable. Land use, precipitation and temperature significantly affected both STN and STP. The effects varied among different precipitation and temperature regions for different land use types. Generally, cropland had higher concentrations and densities of STN and STP than forestland and grassland. Regions with higher precipitation and temperatures had higher STN and STP densities. The values of STN and STP could be predicted by various land-use specific linear models incorporating appropriate combinations of related variables, i.e., soil organic carbon, precipitation, temperature, elevation, latitude, longitude, slope gradient, clay content, silt content and soil pH.

Both STN and STP demonstrated moderate spatial dependence. The spatial ranges of STN and STP ranged from 374 to 461 km and from 546 to 664 km, respectively, which was much larger than the sampling interval, demonstrating that the sampling system used could adequately detect the regional spatial pattern of STN and STP. The distribution maps of STND and STPD in the 0–40 cm soil layer showed similar spatial distributions that basically consisted of an area of low N and P that was surrounded by bands with higher levels that progressively increased towards the region's boundary. Stocks of STN and STP were estimated to be 0.217 Pg and 0.205 Pg, respectively, in the upper 0–40 cm soil layer, which were about 5.4% and 7.3% of the total N and P stocks in China.

This study identified the areas of low and high STN and STP on the Loess Plateau and the factors influencing these levels. It found that it was important to take land use into account when considering variations in STN and STP at the regional scale, but taking climate-based sub-regions into account enhanced the accuracy of model predictions. Hence, further work should be done at sub-regional scales to increase detailed information about spatial variability and land use effects that contribute to the regional framework.

Acknowledgments

This research was supported by the projects of Innovation Team Program of the Chinese Academy of Sciences, the Program for Innovative Research Team of Ministry of Education, China (No. IRT0749), and the National Natural Science Foundation of China (No. 41071156 and No. 51179180). We wish to thank the editor and reviewer for their valuable comments and detailed suggestions. Special thanks also go to Dr. Myroslava Khomik and Mr. David Warrington for their zealous help in improving the manuscript.

References

Batjes, N.H., 1996. Total carbon and nitrogen stocks in the soils of the world. European Journal of Soil Science 47, 151–163.
Bremner, J.M., Tabatabai, M.A., 1972. Use of an ammonia electrode for determination of ammonia in Kjedahl. Analysis 3, 159–165.
Bronson, K., Zobeck, T., Chua, T.T., Acosta-Martinez, V., van Pelt, R.S., Booker, J.D., 2004. Carbon and nitrogen pools of southern high plains cropland and grassland soils. Soil Science Society of America Journal 68, 1695–1704.
Cambardella, C.A., Moorman, T.B., Novak, J.M., Parkin, T.B., Karlen, D.L., Turco, R.F., Konopka, A.E., 1994. Field-scale variability of soil properties in Central Iowa soils. Soil Science Society of America Journal 58, 1501–1511.
Chen, M., Chen, J., Sun, F., 2008. Agricultural phosphorus flow and its environmental impacts in China. Science of the Total Environment 405, 140–152.
Gami, S.K., Lauren, J.G., Duxbury, J.M., 2009. Influence of soil texture and cultivation on carbon and nitrogen levels in soils of the eastern Indo-Gangetic Plains. Geoderma 153, 304–311.
Garten, C.T., Kang, S., Brice, D.J., Schadt, C.W., Zhou, J., 2007. Variability in soil properties at different spatial scales (1 m–1 km) in a deciduous forest ecosystem. Soil Biology and Biochemistry 39, 2621–2627.
Giesler, R., Pettersson, T., Högberg, P., 2002. Phosphorus limitation in boreal forests: effects of aluminum and iron accumulation in the humus layer. Ecosystems 5, 300–314.
Gong, Z.T., 2003. Chinese Soil Taxonomy: Theory, Method, Practice. Science Press, Beijing.
Goovaerts, P., 1999. Geostatistics in soil science: state-of-the-art and perspectives. Geoderma 89, 1–45.
Hageback, J., Sundberg, J., Ostwald, M., Chen, D., Xie, Y., Knutsson, P., 2005. Climate variations and land use in Danangou watershed, China—examples of small-scale farmers' adaptation. Climatic Change 72, 189–212.
Hagedorn, F., Spinnler, D., Siegwolf, R., 2003. Increase N deposition retards mineralization of old soil organic matter. Soil Biology and Biochemistry 35, 1683–1692.
Hassink, J., 1996. Preservation of plant residues in soils differing in unsaturated protective capacity. Soil Science Society of America Journal 60, 487–491.
Hati, K.M., Swarup, A., Mishra, B., Manna, M.C., Wanjari, R.H., Mandal, K.G., Misra, A.K., 2008. Impact of long-term application of fertilizer, manure and lime under intensive cropping on physical properties and organic carbon content of an Alfisol. Geoderma 148, 173–179.
Issaks, E.K., Srivastava, R.M., 1989. An Introduction to Applied Geostatistics. Oxford University Press, New York . (375 pp.).
Jennings, E., Allott, N., Pierson, D.C., Schneiderman, E.M., Lenihan, D., Samuelsson, P., Taylor, D., 2009. Impact of climate change on phosphorus loading from a grassland catchment: implication for future management. Water Research 43, 4316–4326.
Jenny, 1941. Factors of Soil Formation: A System of Quantitative Pedology. McGraw-Hill, New York . (Reprinted by Dover Publications, New York).
Karhu, K., Fritze, H., Tuomi, M., Vanhala, P., Spetz, P., Kitunen, V., Liski, J., 2010. Temperature sensitivity of organic matter decomposition in two boreal forest soil profiles. Soil Biology and Biochemistry 42, 72–82.
Lal, R., 2004. Soil C sequestration impacts on Global Climatic Change and Food Security. Science 304, 1623–1627.
Leifeld, J., Bassin, S., Fuhrer, J., 2005. Carbon stocks in Swiss agricultural soils predicted by land-use, soil characteristics, and altitude. Agriculture, Ecosystems and Environment 105, 255–266.
Lin, J.S., Shi, X.Z., Lu, X.X., Yu, D.S., Wang, H.J., Zhao, Y.C., Sun, W.X., 2009. Storage and spatial variation of phosphorus in paddy soils of China. Pedosphere 19, 790–798.
Liu, G., 1999. Soil conservation and sustainable agriculture on the Loess Plateau: challenges and prospects. Ambio 28, 663–668.
Liu, E., Yan, C., Mei, X., He, W., Bing, S.H., Ding, L., Liu, Q., Liu, S., Fan, T., 2010. Long-term effect of chemical fertilizer, straw, and manure on soil chemical and biological properties in northwest China. Geoderma 158, 173–180.
Liu, Z.P., Shao, M.A., Wang, Y.Q., 2011. Effect of environmental factors on regional soil organic carbon stocks across the Loess Plateau region, China. Agriculture, Ecosystems and Environment 142, 184–194.
Matheron, G., 1963. Principles of geostatistics. Economic Geology 58, 1246–1266.
McLean, E.O., 1982. Soil pH and lime requirement, In: page, A.L., Miller, R.H., Keeney, D.R. (Eds.), Methods of Soil Analysis. Part 2, 2nd ed. Agron. Monogr., vol. 9. ASA and SSSA, Madison, WI, pp. 199–224.
Meersmans, J., De Ridder, F., Canters, F., De Baets, S., Van Molle, M., 2008. A multiple regression approach to assess the spatial distribution of Soil Organic Carbon (SOC) at the regional scale (Flanders, Belgium). Geoderma 143, 1–13.
Moazed, H., Hoseini, Y., Naseri, A.A., Abbasi, F., 2010. Determining phosphorus adsorption isotherm in soil and its relation to soil characteristics. International Journal Soil Science 5, 131–139.
Murphy, J., Riley, J.P., 1962. A modified single solution method for the determination of phosphate in natural water. Analytica Chimica Acta 27, 31–36.
Nelson, D.W., Sommers, L.E., 1982. Total carbon, organic carbon and organic matter, In: Page, A.L., Miller, R.H., Keeney, D.R. (Eds.), Methods of Soil Analysis, Part 2, 2nd edition. Agronomy Monograph, vol. 9. ASA and SSSA, Madison, WI, pp. 534–580.
Nielsen, D.R., Bouma, J., 1985. Soil Spatial Variability. Pudoc, Wageningen.
Ostwald, M., Chen, D., 2006. Land-use change: impacts of climate variation and policies among small-scale farmers in the Loess Plateau, China. Land Use Policy 23, 361–371.
Patil, R.H., Laegdsmand, M., Olesen, J.E., Porter, J.R., 2010. Effect of soil warming and rainfall patterns on soil N cycling in Northern Europe. Agriculture, Ecosystems and Environment 139, 195–205.
Post, W.M., Pastor, J., Zinke, P.J., Stangenberger, A.G., 1985. Global patterns of soil nitrogen storage. Nature 317, 613–616.
Quilchano, C., Marañón, T., Pérez-Ramos, I.M., Noejovich, L., Valladares, F., Zavala, M.A., 2008. Patterns and ecological consequences of abiotic heterogeneity in managed cork oak forests of Southern Spain. Ecological Research 23, 127–139.
Rezaei, S.A., Gilkes, R.J., 2005. The effects of landscape attributes and plant community on soil chemical properties in rangelands. Geoderma 125, 167–176.
Rodríguez, A., Durán, J., Fernández-Palacios, J.M., Gallardo, A., 2009. Spatial pattern and scale of soil N and P fractions under the influence of a leguminous shrub in a *Pinus canariensis* forest. Geoderma 151, 303–310.
Ross, D.J., Tate, K.R., Scott, N.A., Feltham, C.W., 1999. Land-use change: effects on soil carbon, nitrogen and phosphorus pools and fluxes in three adjacent ecosystems. Soil Biology and Biochemistry 31, 803–813.
Sediment Specialty Committee of Chinese Water Resources Association, 1989. The Handbook of Sediment. The Chinese Environment Science Press . (in Chinese).
Shi, H., Shao, M.A., 2000. Soil and water loss from the Loess Plateau in China. Journal of Arid Environments 45, 9–20.
Smil, V., 2000. Phosphorus in the environment: natural flows and human interferences. Annual Review of Energy and the Environment 25, 53–58.
Tan, Z.X., Lal, R., Smeck, N.E., Calhoun, F.G., 2004. Relationship between surface soil organic carbon pool and site variables. Geoderma 121, 187–195.
Tang, K.L., 1991. Soil Erosion on the Loess Plateau: Its Regional Distribution and Control. China Sciences and Technology Press, Beijing . (in Chinese).
Tian, H.Q., Wang, S.Q., Liu, J.Y., Pan, S.F., Chen, H., Zhang, C., Shi, X.Z., 2006. Patterns of soil nitrogen storage in China. Global Biogeochemical Cycles 20, GB1001 http://dx.doi.org/10.1029/2005GB002464.
Trangmar, B.B., Yost, R.S., Uehara, G., 1985. Application of geostatistics to spatial studies of soil properties. Advances in Agronomy 38, 45–94.
Vitousek, P.M., Cassman, K., Cleveland, C., Crews, T., Field, C.B., Grimm, N.B., Howarth, R.W., Marino, R., Martinelli, L., Rastetter, E.B., Sprent, J.I., 2002. Towards an ecological understanding of biological nitrogen fixation. Biogeochemistry 57 (58), 1–45.
Wang, S.P., Zhou, G.S., Gao, S.H., Guo, J.P., 2005. Gradient distribution of soil nitrogen and its response to climate change along the Northeast China Transect. Chinese Journal of Applied Ecology 16, 279–283 (in Chinese with English abstract).
Wang, G.P., Liu, J.S., Wang, J.D., Yu, J.B., 2006. Soil phosphorus forms and their variations in depressional and riparian freshwater wetlands (Sanjiang Plain, Northeast China). Geoderma 132, 59–74.
Wang, Y.Q., Zhang, X.C., Huang, C.Q., 2009. Spatial variability of soil total nitrogen and soil total phosphorus under different land uses in a small watershed on the Loess Plateau, China. Geoderma 150, 141–149.

Wang, Y.F., Fu, B.J., Lv, Y.H., Song, C.J., Luan, Y., 2010. Local-scale spatial variability of soil organic carbon and its stock in the hilly area of the Loess Plateau, China. Quaternary Research 73, 70–76.
Wang, Y.Q., Shao, M.A., Zhu, Y.J., Liu, Z.P., 2011. Impact of land use and plant characteristics on dried soil layers in different climatic regions on the Loess Plateau of China. Agricultural and Forest Meteorology 151, 437–448.
Webster, R., Oliver, M.A., 2000. Geostatistics for Environmental Scientists. Wiley, Chichester . (271 pp.).
Yamamoto, J.K., 2005. Correcting the smoothing effect of ordinary kriging estimates. Mathematical Geology 37 (1), 69–94.
Yang, W.Z., Shao, M.A., 2000. Soil Water Research on the Loess Plateau. Science Press, Beijing . (in Chinese with English abstract).
Yang, Y.H., Ma, W.H., Mohammat, A., Fang, J.Y., 2007. Storage, patterns and controls of soil nitrogen in China. Pedoshpere 17, 776–785.
Zhang, C., Tian, H.Q., Liu, J.Y., Wang, S.Q., Liu, M.L., Pan, S.F., Shi, X.Z., 2005. Pools and distribution of soil phosphorus in China. Global Biogeochemical Cycles 19, GB1020 http://dx.doi.org/10.1029/2004GB002296.
Zhang, S.L., Yang, X.Y., Wiss, M., Crip, H., Lovdahl, L., 2006. Changes in physical properties of a loess soil in China following two long-term fertilization regimes. Geoderma 136, 579–587.
Zheng, F., He, X., Gao, X., Zhang, C., Tang, K., 2005. Effects of erosion patterns on nutrient loss following deforestation on the Loess Plateau of China. Agriculture, Ecosystems and Environment 108, 85–97.